*International Journal of Thermophysics, Vol. 22, No. 5, September 2001 (© 2001)*

# An Effective Emissivity Model for Rapid Thermal Processing Using the Net-Radiation Method[1]

**Z. M. Zhang[2, 3] and Y. H. Zhou[2]**

A reflective shield has been placed in the lower chamber of some rapid thermal processing (RTP) systems so that the temperature of the silicon wafer can be accurately measured *in situ* with light-pipe radiometers. Better knowledge of the effective emissivity of the wafer reduces the uncertainty in the temperature measurement. This paper describes an enclosure model based on the net-radiation method for predicting the effective emissivity of the wafer. The model treats the surfaces in the enclosure as diffuse emitters, with a reflectivity that may include a diffuse component and a specular component. Using this model, a parametric study is performed to investigate the influence of the geometric arrangement, surface temperature and properties, and wavelength on the effective emissivity. The algorithm developed in this work may serve as a tool to improve radiometric temperature measurement in RTP systems.

**KEY WORDS:** effective emissivity; enclosure model; net-radiation method; radiometric temperature measurement; rapid thermal processing.

## 1. INTRODUCTION

As the packing density continues to increase and feature sizes continue to shrink in microelectronics, rapid thermal processing (RTP) has become a key technology in semiconductor device fabrication. In an RTP furnace, the wafer is individually heated by optical radiation, to temperatures as high as 1100°C in about 10 s, in contrast to the 30-min typical ramp time in batch furnaces. The short ramp time prevents the ions from diffusing too far into the silicon, allowing the feature size to be minimized. Accurate

[1] Paper presented at the Fourteenth Symposium on Thermophysical Properties, June 25–30, 2000, Boulder, Colorado, U.S.A.

[2] Department of Mechanical Engineering, University of Florida, Gainesville, Florida 32611, U.S.A.

[3] To whom correspondence should be addressed. E-mail: zzhang@cimar.me.ufl.edu



0195-928X/01/0900-1563/0 © 2001 Plenum Publishing Corporation

determination of the wafer temperature is a challenging issue for RTP and thus has attracted the attention of many researchers [1–5]. Radiometric thermometry based on sapphire light pipes (or optical fibers) is the method of choice for *in situ* temperature monitoring. Because the radiometer output is proportional to the exitent (i.e., emitted plus reflected) radiance from the target, the emissivity and the surrounding radiation must be well characterized [5, 6]. The emissivity of the wafer is a function of wavelength and temperature and can vary over a large range due to dopant type and concentration, surface roughness, coating layers, and patterning [4–10]. A reflective shield has been placed in the lower chamber of some RTP systems to enhance the effective emissivity of the wafer, thus reducing the temperature measurement uncertainty [11, 12]. Knowledge of the effective emissivity of the wafer is required to correlate the measured radiance temperature to the surface temperature.

In the past, Bedford and Ma [13] performed a series of studies to calculate the local, hemispherical effective emissivity of diffuse cavities based on the zonal approximation of the integral equations, which were solved iteratively. Chu et al. [14] later extended this method to include a specularly reflecting lid. Monte Carlo methods have also been used extensively to predict the effective emissivity of cavities [15–17]. Monte Carlo methods can incorporate complex directional distributions of the radiative properties of the surfaces involved and may be used to evaluate the directional effective emissivity. Since a large number of ray bundles is required to achieve the desired accuracy, Monte Carlo simulation often takes a large amount of computation time.

Recently, the net-radiation method was employed to study the lower chamber of the RTP furnace at the National Institute of Standards and Technology (NIST) [12, 18]. The enclosure was divided into small surface elements, whose radiosities were calculated without any iteration by solving a matrix equation. In the present paper, we describe a somewhat general formulation of this model that, in principle, can incorporate partially diffuse and partially specular surfaces and demonstrate the influence of various parameters on the effective emissivity. The objective is to develop a robust and convenient tool for radiometric temperature measurement in RTP systems.

Our model is based on NIST's RTP test bed [12], whose lower chamber may be regarded as a cylindrical enclosure that consists of a silicon wafer with a guard ring as the top surface, a reflective shield (over a cold plate) as the bottom surface, and a guard tube as the lateral surface (see Fig. 1). The light pipe views a small portion of the wafer through an opening (i.e., radiometer hole) at the center of the shield. The wafer is supported by three 2-mm-diameter alumina rods, which are neglected in

the present model. Some additional holes on the shield are also neglected to make the model axisymmetric. The radius of the wafer is 100 mm, and that of the shield is 135 mm. The distance between the wafer and the shield ($L$) is taken as a variable with a typical value of 12.5 mm. The narrow-band filter radiometer used at NIST has a central wavelength of $\lambda = 0.955$ $\mu$m. The emissivity $\varepsilon_{\lambda,\mathrm{w}}$ of lightly doped silicon at 800°C is approximately 0.65 [12].

## 2. ANALYSIS

For an enclosure consisting of $N$ opaque surfaces, when the emitted radiation is diffuse and the reflected radiation is composed of a diffuse component and a specular component, the spectral directional-hemispherical reflectivity ($\rho_\lambda$) and the spectral hemispherical emissivity ($\varepsilon_\lambda$) of each surface are related by

$$\rho_\lambda = \rho_\lambda^{\mathrm{d}} + \rho_\lambda^{\mathrm{s}} = 1 - \varepsilon_\lambda \tag{1}$$

where superscripts d and s denote, respectively, the diffuse and specular components. It is assumed that $\rho_\lambda^{\mathrm{d}}$ and $\rho_\lambda^{\mathrm{s}}$ are also independent of the angle of incidence. The specular view factor (also called exchange factor), $F_{i-j}^{\mathrm{s}}$, between surface $A_i$ and surface $A_j$ is defined as the fraction of diffuse radiant energy leaving $A_i$ that reaches $A_j$ by direct travel and by a number of specular reflections [19–21]. The portion that accounts for direct travel is the regular (diffuse) view factor, $F_{i-j}$. The contribution of specular reflection is the view factor between $A_i$ and each of $A_j$'s virtual surfaces multiplied by the corresponding specular reflectivities of the surfaces that image $A_j$. For the simple enclosure shown in Fig. 1, if only the reflective shield contains a specular component with a uniform reflectivity over the entire shield (neglecting the radiometer hole), virtual surfaces that image the wafer, guard ring, and guard tube can be created below the shield. Similarly, if the reflectivities of the wafer and the guard ring are the same and include a specular component, while the guard tube and shield are diffuse reflectors, then virtual surfaces of the shield and guard tube can be created above the wafer and the guard ring.

If the temperature and the spectral radiative properties of each surface for a given enclosure are prescribed, the net-radiation method can be applied to yield the following set of equations [19, 20]:

$$\sum_{j=1}^{N} \left[\delta_{ij} - \rho_{\lambda,i}^{\mathrm{d}} F_{i-j}^{\mathrm{s}}\right] J_{\lambda,j} = \varepsilon_{\lambda,i} E_{\lambda\mathrm{b},i}, \qquad i = 1, 2, \ldots, N \tag{2}$$

where $\delta_{ij}$ is Kronecker's delta function ($\delta_{ij} = 1$ if $i = j$ and $\delta_{ij} = 0$ if $i \neq j$), $E_{\lambda b}$ is the blackbody spectral emissive power given by Planck's law and is a function of the surface temperature, and $J_\lambda$ is the spectral (diffuse) radiosity, which includes emitted and diffusely reflected radiation from the surface, since specular reflections are accounted for by the exchange factors. The $N$ linear equations can be solved using the standard matrix-inversion method to obtain $J_{\lambda,i}$ ($i = 1, 2,..., N$) for any given wavelength. If $H_{\lambda,i}$ is the spectral irradiation (i.e., incoming heat flux) from the enclosure to its $i$th surface, then

$$J_{\lambda,i} = \varepsilon_{\lambda,i} E_{\lambda b,i} + \rho^{d}_{\lambda,i} H_{\lambda,i} \tag{3}$$

For diffuse surfaces ($\rho^{s}_{\lambda} = 0$), the radiosity is the sum of the emitted and reflected radiant heat fluxes leaving the surface, whereas for specular surfaces ($\rho^{d}_{\lambda} = 0$), the radiosity consists of only the emitted radiant heat flux. The spectral irradiation may be approximated by

$$H_{\lambda,i} = \sum_{j=1}^{N} J_{\lambda,j} F^{s}_{i-j}, \qquad i = 1, 2,..., N \tag{4}$$

where the reciprocal relation $A_i F^{s}_{i-j} = A_j F^{s}_{j-i}$ has been used. The net spectral radiant heat flux leaving surface $A_i$ is

$$q_{\lambda,i} = \varepsilon_{\lambda,i} (E_{\lambda b,i} - H_{\lambda,i}) \tag{5}$$

The effective emissivity of a surface is defined as the ratio of the radiant energy leaving that surface by emission and reflection (both diffusely and specularly) to that of a blackbody at the same temperature. Hence, the local (spectral hemispherical) effective emissivity for the $i$th surface is

$$\varepsilon_{\lambda eff,i} = [\varepsilon_{\lambda,i} E_{\lambda b,i} + (1 - \varepsilon_{\lambda,i}) H_{\lambda,i}] / E_{\lambda b,i} \tag{6}$$

The integration of $q_{\lambda,i}$ over all wavelengths yields the net radiant heat flux from the $i$th surface. The total radiative property is the integral of the product of the corresponding spectral property and $E_{\lambda b}$ divided by $E_b$ (the total blackbody emissive power given by the Stefan–Boltzmann law). If all the radiative properties are independent of wavelength (i.e., under the gray-body assumption), then the subscript $\lambda$ in Eqs. (2) through (6) can be eliminated. In this case, the total hemispherical effective emissivity of the $i$th surface becomes

$$\varepsilon_{eff,i} = [\varepsilon_i E_{b,i} + (1 - \varepsilon_i) H_i] / E_{b,i} \tag{7}$$

Furthermore, if $\rho_\lambda^s = 0$ for all surfaces, then $F_{i-j}^s \equiv F_{i-j}$ and the expressions above reduce to the corresponding equations for diffuse-gray enclosures.

It is worth noting that for an enclosure of gray surfaces for which the emissivity and reflectivity are independent of wavelength, $\varepsilon_{\lambda,\text{eff}}$ is, in general, wavelength dependent and different from $\varepsilon_{\text{eff}}$ because $H_{\lambda,i}$ is a complicated function of $\lambda$ and the temperature and properties of each surface [13].

In the present model, the first surface element on the wafer is a disk with a radius equal to that of the radiometer view spot (surface 1 in Fig. 1), and the first surface element on the reflective shield is the 2-mm-radius disk that represents the radiometer hole (i.e., the light pipe and the sheath). The radius of the view spot on the wafer depends on the radius of the light pipe, the distance $L$ separating the shield from the wafer, and the beam divergence. The simple relation given in Ref. 12, $1+(L/3)$ (mm), is used here. The guard ring and the rest of the wafer are divided into concentric rings of approximately equal radial increment. The rest of the shield is also divided into concentric rings. The guard tube is not divided into smaller surface elements. The number of surface elements on the shield is equal to the total number of surface elements on the wafer, the guard ring, and the guard tube. The view factor between coaxial parallel rings or between a coaxial ring and the tube can be obtained from the view factor between coaxial parallel disks using the view factor algebra [21].

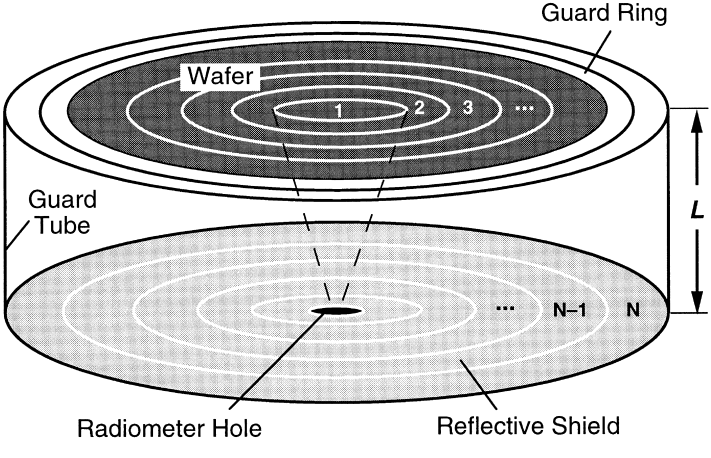


**Fig. 1.** Schematic of the enclosure model of the lower chamber of RTP systems.

Although the temperatures and radiative properties of the surface elements can be individually assigned, they are assumed to be uniform in each zone, that is, the wafer, the guard ring, the guard tube, the radiometer hole, and the rest of the shield. The temperature of the wafer is assumed to be 800°C, and the temperatures of the shield, radiometer hole, and guard tube are assumed to be 27°C for most calculations. Two cases are considered with regard to the conditions of the guard ring. In the first case the guard ring is at 27°C and has a low spectral-hemispherical emissivity ($\varepsilon_{\lambda,\mathrm{r}}=0.1$), corresponding to a cold guard ring made of platinum-coated quartz [12]. In the second case it is at the same temperature and has the same emissivity as the wafer, to simulate the guard ring made of silicon [11]. The reflectivity of the gold-plated reflective shield can be as high as 0.993 ($\varepsilon_{\mathrm{s}}=0.007$). The emissivity of the hole is assumed to be 0.925, based on the refractive index of sapphire at 0.955 $\mu$m [22]. The effect of the radiometric hole is studied by comparing the results obtained with an emissivity of 0.925 and with an emissivity equal to that of the shield.

Although Eqs. (1) through (7) are applicable to an infinite series of virtual surfaces, the determination of the specular view factor is very complex considering multiple specular reflections. Since the purpose of this work is to develop a simple model, it is assumed that only the top or bottom surface may include specular components. When $\rho_\lambda^{\mathrm{s}}$ of the wafer is not zero, $\rho_\lambda^{\mathrm{d}}$ and $\rho_\lambda^{\mathrm{s}}$ of the guard ring and wafer are set to be the same. Similarly, the properties of the radiometer hole and the shield are assumed to be the same when the shield includes specular reflection.

The effect of the number of surface elements was investigated, and the calculated effective emissivity was found to converge to within 0.0005 when the wafer was divided into 20 surface elements. In all our calculations, the wafer is divided into 40 surface elements to produce a smooth curve, and the guard ring is divided into 12 surface elements. It takes only a few seconds on a personal computer to run one test.

## 3. RESULTS AND DISCUSSION

The spectral hemispherical effective emissivity of the wafer at $\lambda=0.955\ \mu$m is shown in Fig. 2 as a function of the distance from the center of the wafer under a variety of conditions. The local effective emissivity away from the center is a useful concept when the light pipe views the wafer at an oblique angle. The temperature and emissivity of the diffuse wafer are $T_{\mathrm{w}}=800$°C and $\varepsilon_{\lambda,\mathrm{w}}=0.65$, respectively. The temperature and emissivity of the shield are $T_{\mathrm{s}}=27$°C and $\varepsilon_{\lambda,\mathrm{s}}=0.007$, respectively (i.e., the reflectivity of the shield is $\rho_{\lambda,\mathrm{s}}=0.993$). The temperature of the guard tube is fixed at $T_{\mathrm{t}}=27$°C, and the distance between the wafer and the shield is

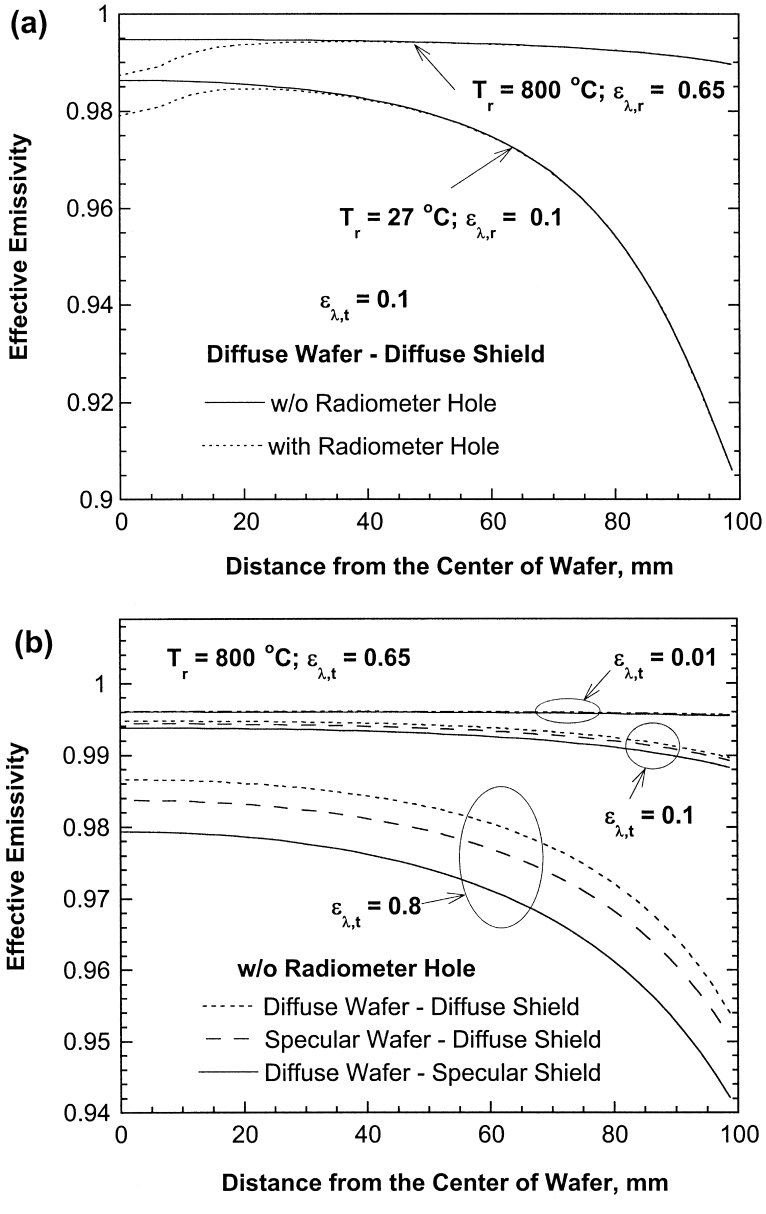


**Fig. 2.** Spectral hemispherical effective emissivity (at $\lambda = 0.955$ $\mu$m) distribution, when $T_w = 800°C$, $T_s = T_t = 27°C$, $\varepsilon_{\lambda,w} = 0.65$, $\varepsilon_{\lambda,s} = 0.007$ and $L = 12.5$ mm. (a) The effects of the radiometer hole and guard ring; (b) the effect of the guard tube.

set at $L = 12.5\ \mu$m. Other parameters of the guard ring, guard tube, and radiometer hole are varied. As shown in Fig. 2a, the conditions of the guard ring have a strong influence on the effective emissivity distribution, especially near the edge of the wafer. The effective emissivity of the wafer becomes much more uniform when the temperature and emissivity of the guard ring approach those of the wafer. The net radiant heat flux (not shown) from the wafer has a distribution similar to that of the (total) effective emissivity. Calculations also show that, for $T_r = 27$°C, an increase in $\varepsilon_r$ can only reduce the effective emissivity of the wafer. The existence of the radiometric hole reduces the effective emissivity in the central region because of its high emissivity (0.925). The influence of the hole is extended to a polar angle of about 60° viewed from the center of the hole (i.e., 22 mm from the center of the wafer). Attention should be paid to the minimization of the radiometer hole in the design of the light-pipe probe. The experimental effective emissivity at the center of the wafer obtained by comparison between a light-pipe radiation thermometry and thin-film thermocouples was approximately 0.98 [12], which is close to the predicted effective emissivity (with a cold guard ring).

The effect of the guard tube emissivity is demonstrated in Fig. 2b, without considering the radiometric hole. The temperature and properties of the guard ring are assumed to be the same as those of the wafer. When the emissivity of the guard tube is very low ($\varepsilon_{\lambda,t} = 0.01$), it acts like a perfect reflector and the effective emissivity of the wafer is then quite uniform in all three cases. This is the most desirable situation for temperature measurements and for the control of temperature uniformity on the wafer. As the emissivity of the guard tube ($\varepsilon_{\lambda,t}$) is increased to 0.8, the effective emissivity of the wafer decreases significantly. Furthermore, the effective emissivity is lowest with a specular shield. When the distance between the wafer and the shield is reduced, the effect of the guard tube emissivity on the effective emissivity at the center of the wafer decreases.

Figure 3 illustrates the wavelength dependence of the effective emissivity of the wafer when all surfaces are assumed to be diffuse and the effect of the radiometer hole is neglected. Assuming that the emissivity of each surface does not depend on the wavelength, the spectral effective emissivity at the center of the wafer is calculated at several different wavelengths and plotted together with the total effective emissivity calculated using the gray model. Note that above 600°C, the emissivity of silicon is between 0.65 and 0.75 in the wavelength range from 1 to 10 $\mu$m [6]. However, below 600°C, lightly doped silicon is semitransparent for a wavelength longer than the band gap of silicon (about 1.1 $\mu$m at room temperature and shifting toward longer wavelengths as the temperature increases). The purpose of Fig. 3 is to show the effect of $T_s$ and $T_t$ on the effective emissivity of the wafer. The

temperature and properties of the guard ring are assumed to be the same as those of the wafer, while the temperature and properties of the guard tube are assumed to be the same as those of the shield. At short wavelengths, the radiant energy emitted from the shield is much lower than that from the wafer when $T_s \ll T_w$. The effective emissivity is the same for all wavelengths when $T_s$ approaches absolute zero. As $T_s$ is getting close to $T_w$, its effect becomes stronger, especially for long wavelengths, owning to the nature of the Planck distribution. Therefore, the effective emissivity is higher at longer wavelengths. When $T_s = T_w$ (i.e., in the case of thermal equilibrium), the effective emissivity becomes unity, regardless of the wavelength. Selecting the most suitable wavelength is important for radiometric temperature measurements.

Figure 4 shows the effects of wafer emissivity and shield emissivity on the effective emissivity at the center of the wafer, without considering the radiometer hole. The temperature of the wafer is assumed to be 800°C, and all other surfaces are assumed to be at 27°C. The magnitude of the wafer temperature is not important as long as it is much higher than that of the

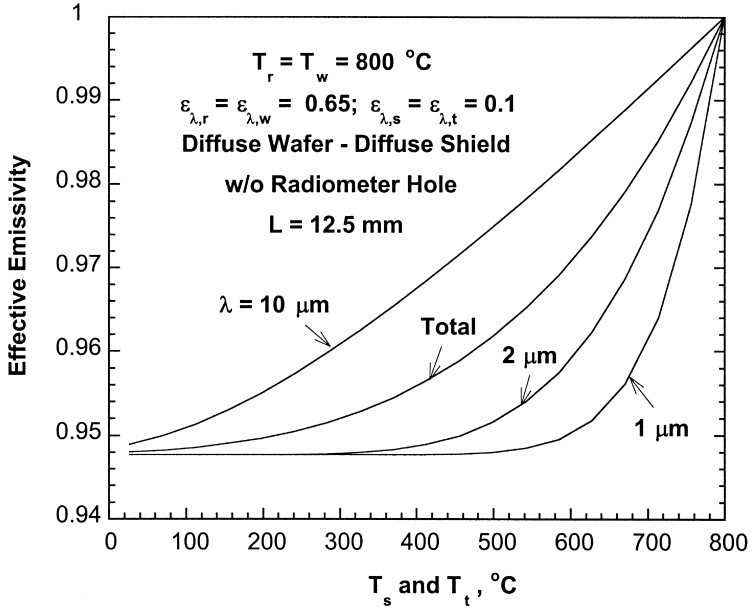


**Fig. 3.** Spectral and total hemispherical effective emissivities at the center of the wafer versus the temperature of the shield ($T_s$) and the tube ($T_t$), assuming that $T_s = T_t$.

rest of the enclosure surfaces. The emissivities of the guard ring and guard tube are assumed to be the same (i.e., $\varepsilon_{\lambda,\mathrm{r}} = \varepsilon_{\lambda,\mathrm{t}} = 0.1$). It can be seen that a specular shield results in a slightly lower effective emissivity compared with a diffuse shield. For a specular shield with an emissivity of 0.007, the effective emissivity of the wafer is 0.9 for $\varepsilon_{\lambda,\mathrm{w}} = 0.3$ and 0.96 for $\varepsilon_{\lambda,\mathrm{w}} = 0.5$. If the wafer emissivity is determined to be 0.65 with an uncertainty of 0.01 (i.e., $\varepsilon_{\lambda,\mathrm{w}} = 0.65 \pm 0.01$), the effective emissivity of the wafer for a specular shield ($\varepsilon_{\lambda,\mathrm{s}} = 0.007$) is $0.981 \pm 0.001$. This can substantially reduce the uncertainty in the determination of the surface temperature from the measured radiance temperature. As shown in Fig. 2a, the effective emissivity of the wafer is higher when the guard ring has the same temperature and emissivity as the wafer. The radiometer hole, however, may reduce the effective emissivity.

The effect of the distance ($L$) between the wafer and the shield was investigated, and the results are shown in Fig. 5 for the diffuse wafer and diffuse shield. The emissivity of the wafer is 0.65, and the radiometer hole is included in some cases. The temperature and emissivity of the guard ring are varied. As $L$ approaches 0, the resulting effective emissivity becomes the same as that predicted from the two-infinite-parallel-plate model

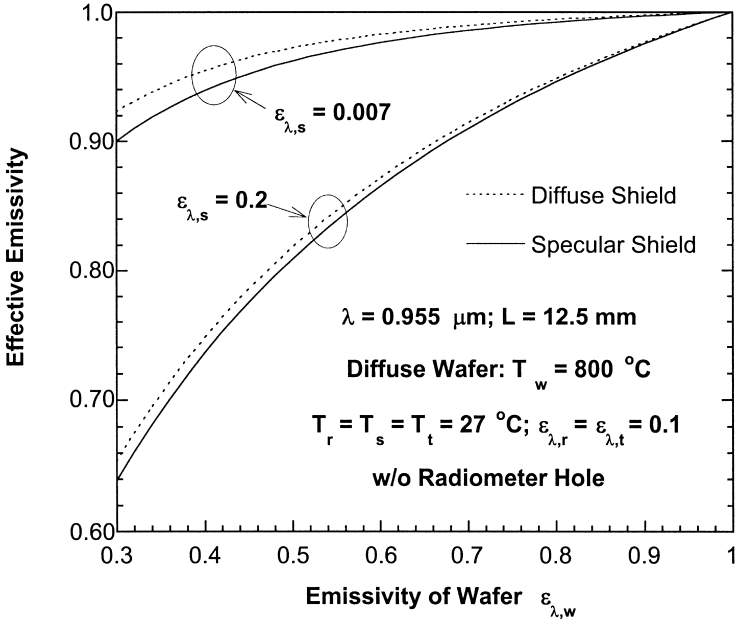


**Fig. 4.** The effects of wafer emissivity and shield emissivity on the spectral hemispherical effective emissivity at the center of the wafer.

[5, 18]. With the radiometer hole, however the effective emissivity is nearly the same as the emissivity of bare silicon, owing to the high emissivity of the hole (0.925). As $L$ increases, the effect of the radiometer hole decreases and the effective emissivity predicted with the hole approaches that without the hole. With a cold guard ring, the effective emissivity decreases as $L$ increases further.

It should be noted that the irradiation is, in general, not diffuse except under the condition of thermal equilibrium. If the wafer is not diffuse, the effective emissivity will depend on the direction. The directional effective emissivity may be needed for light-pipe measurements. The net-radiation method is limited to predicting the hemispherical effective emissivity. The Monte Carlo method can be used to calculate the directional effective emissivity and to include more complex surface properties, such as the bidirectional reflectance distribution function (BRDF) [23], with the requirement of a long computational time. A Monte Carlo model developed for the RTP chamber has been presented in a separate paper [24]. The model presented here, based on the net-radiation method, is

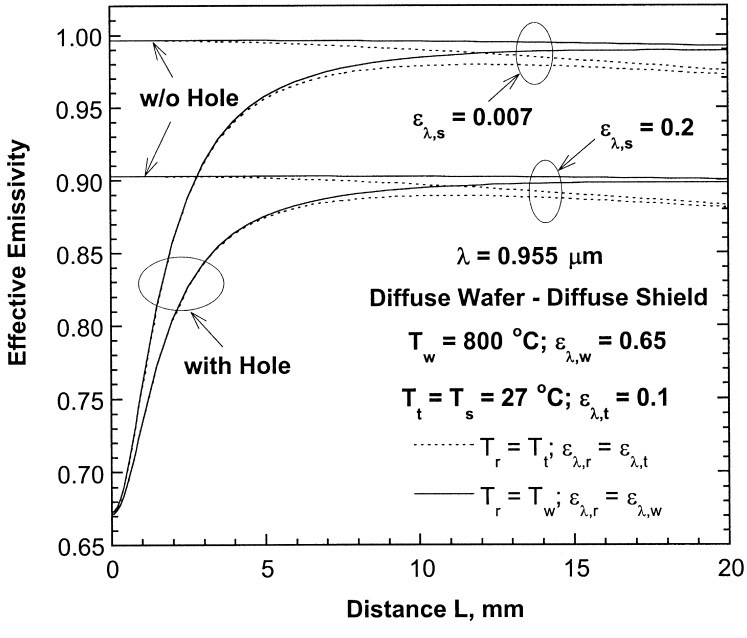


**Fig. 5.** Spectral hemispherical effective emissivity at the center of the wafer versus the distance between the wafer and the shield.

advantageous in terms of convenience and speed. It can be used for selecting light-pipe radiometers, for correlating the radiometer reading with the surface temperature, and for analyzing heat transfer in RTP systems. It may serve as a basis to validate the more complicated Monte Carlo model.

## 4. CONCLUSIONS

A convenient effective emissivity model has been developed and is recommended for use as a tool for radiometric temperature measurement and heat transfer analysis in RTP systems. The temperature and properties of the guard ring have a strong influence on the local effective emissivity of the wafer, especially away from the center. If the guard tube is kept at a temperature much lower than that of the wafer, it should be covered with a highly reflective coating. The opening of the radiometer hole needs to be taken into consideration in evaluating the effective emissivity of the wafer for light-pipe thermometry. Research is under way to examine the directional effect using the Monte Carlo method and to apply the modeling results to RTP temperature measurements.

## ACKNOWLEDGMENTS

This work was supported by National Institute of Standards and Technology (NIST) Grant 70-NANB-8H0011 and National Science Foundation Grant CTS-9875441. The authors thank David DeWitt and Benjamin Tsai of the NIST and Ferdinand Rosa (a former graduate student of the University of Florida) for valuable discussions.

## REFERENCES

1. F. Roozeboom, *J. Vac. Sci. Technol. B* **8**:1249 (1990).
2. P. J. Timans, *Mater. Sci. Semicond. Process.* **1**:169 (1998).
3. F. Roozeboom (ed.), *Advances in Thermal and Integrated Processing* (Kluwer Academic, Dordrecht, 1996).
4. P. J. Timans, *Solid State Technol.* **40**:63 (1997).
5. D. P. DeWitt, F. Y. Sorrel, and J. K. Elliott, *Mater. Res. Soc. Symp. Proc.* **470**:3 (1997).
6. Z. M. Zhang, in *Annual Review of Heat Transfer*, C. L. Tien, ed. (Begell House, New York, 2000), Vol. 11, Chap. 6.
7. P. Vandenabeele and K. Maex, *J. Appl. Phys.* **72**:5967 (1992).
8. P. Y. Wong, C. K. Hess, and I. N. Miaoulis, *Opt. Eng.* **34**:1776 (1995).
9. J. P. Hebb and K. F. Jensen, *J. Electrochem. Soc.* **143**:1142 (1996).
10. N. M. Ravindra, S. Abedrabbo, W. Chen, F. M. Tong, A. K. Nanda, and A. C. Speranza, *IEEE Trans. Semicond. Manuf.* **11**:30 (1998).
11. A. Acharya and P. J. Timans, *Mater. Res. Soc. Symp. Proc.* **525**:21 (1998).

12. B. K. Tsai and D. P. DeWitt, in *Seventh Int. Conf. Adv. Therm. Process. of Semicond.–RTP '99*, Colorado Springs, CO (1999), pp. 125–135; C. W. Meyer, D. W. Allen, D. P. DeWitt, K. G. Kreider, F. L. Lovas, and B. K. Tsai, in *RTP '99*, pp. 136–141.
13. R. E. Bedford and C. K. Ma, *J. Opt. Soc. Am.* **64**:339 (1974); **65**:565 (1975); **66**:724 (1976).
14. Z. Chu, Y. Sun, R. E. Bedford, and C. K. Ma, *Appl. Opt.* **25**:4343 (1986).
15. A. Ono, *J. Opt. Soc. Am.* **70**:547 (1980).
16. Z. Chu, J. Dai, and B. E. Bedford, in *Temperature, Its Measurement and Control in Science and Industry* (American Institute of Physics, New York, 1992), Vol. 6, pp. 907–912.
17. V. I. Sapritsky and A. V. Prokhorov, *Metrologia* **29**:9 (1992).
18. F. Rosa, Y. H. Zhou, Z. M. Zhang, D. P. DeWitt, and B. K. Tsai, in *Advanced in Rapid Thermal Processing*, F. Roozeboom, J. C. Gelpey, M. C. Öztürk, and J. Nakos, eds. (Electrochemical Society, Pennington, NJ, 1999), Proc. Vol. 99–10, pp. 419–426.
19. M. F. Modest, *Radiative Heat Transfer* (McGraw–Hill, New York, 1993), Chaps. 4–7.
20. E. M. Sparrow and R. D. Cess, *Radiation Heat Transfer*, augmented ed. (Hemisphere, Washington, DC, 1978), Chap. 5.
21. R. Siegel and J. R. Howell, *Thermal Radiation Heat Transfer*, 3rd ed. (Hemisphere, Washington, DC, 1992), Chaps. 6–9.
22. F. Gervais, in *Handbook of Optical Constants of Solids*, E. D. Palik, ed. (Academic Press, San Diego, 1998), Vol. 2, pp. 761–776.
23. Y. J. Shen, Z. M. Zhang, B. K. Tsai, and D. P. DeWitt, *Int. J. Thermophys.* **22**:1311 (2001).
24. Y. H. Zhou, Y. J. Shen, Z. M. Zhang, B. K. Tsai, and D. P. DeWitt, in *Eighth Int. Conf. Adv. Therm. Process. Semicond.–RTP '00*, Gaithersburg, MD (2000), pp. 94–103.